7th International Conference on Computational and Mathematical Biomedical Engineering - CMBE2021
27–29 June 2022, Italy
P. Nithiarasu and C. Vergara (Eds.)

GROWTH AND REMODELLING OF RIGHT VENTRICLE UNDER PULMONARY ARTERIAL HYPERTENSION

Debao Guan[1], Lian Tian[2], and Hao Gao[1]
[1]School of Mathematics and Statistics, University of Glasgow, UK,
{debao.guan,hao.gao}@glasgow.ac.uk
[2]Strathclyde Institute of Pharmacy and Biomedical Sciences, University of Strathclyde, UK,
lian.tian@strath.ac.uk

SUMMARY

Pulmonary arterial hypertension (PAH) is a fatal and rapidly progressive disease, and right ventricular failure is the main cause of death in patients with PAH. This study aims to determine the mechanical cues that can trigger growth and remodelling of heart. To this end, two bi-ventricular models of a control rat heart and a diseased rat heart with PAH are reconstructed, respectively, then the growth amount is estimated by warping the PAH heart to the control heart. Finally, correlation analysis between mechanical cues (stress and strain) and growth tensors demonstrates principal strain may be a triggering cue for the myocardial growth under PAH.

Key words: *pulmonary arterial hypertension, growth and remodelling, rat heart*

1 INTRODUCTION

Pulmonary arterial hypertension (PAH) is a fatal and rapidly progressive disease with a median survival of 2.8 years if untreated. As PAH progresses, right ventricle (RV) undergoes significant growth and remodelling (G&R), such as hypertrophy, dilatation and fibrosis, and eventually fails to pump sufficient blood into the pulmonary arteries, leading to death eventually. It is believed that the imbalanced mechanical environment under PAH plays a critical role in triggering RV G&R, while few studies have been focused on RV [1], which has historically received little attention from the medical and scientific communities though we appreciate RV is equally essential as the left ventricle [2]. Thus, there is an urgent need to develop mathematical models for RV biomechanics.

This study aims to develop experiment-informed G&R models to provide new insights into the consequences of mechanobiology (strain/stress-driven) in RV failure under PAH for deciphering the onset of adverse growth and remodelling (G&R) using the controlled rat experiments. Until now, simplified rat heart models with preserved main anatomical structures are reconstructed from ultrasound images, in which the left ventricle (LV) is included to provide the support of RV dynamics. The anatomical change of RV at different stages is further qualitatively computed through a large deformation diffeomorphic mapping algorithm, which will be used for informing G&R laws. The preliminary results show that the biomechanical RV-LV model at different PAH stages matches well in vivo pressure-volume loops and echocardiographic wall motions. Estimated growth amounts by comparing normal and PAH hearts show that growth mainly occurs at RV free wall (RVFW) while nearly no growth in the septum. The correlation analysis shows that stress and strain both play an important role in G&R, with high correlations with principal strain and active tension.

2 METHODOLOGY

2.1 Animal model of PAH and acquisition of in vivo data

To develop PAH of animal models, male Sprague Dawley rats received a single subcutaneous injection of monocrotaline (MCT; 60 mg/kg). Control rats received phosphate-buffered saline (PBS; 2 mL/kg).

In week 4 post-injection, MCT rats developed severe PAH. In vivo pressure-volume data were obtained via cardiac catherization in closed-chest rats using a micromanometer with high-fidelity 1.9-F rat pressure-volume catheter (Transonic, London, ON, Canada) as described [3]. Ultrasound images of long- and short-axis views of the hearts were obtained using a high-frequency ultrasound system (Vevo 2100; Visual Sonics, Toronto, ON, Canada) as shown in Figure 1, where a control rat heart and an MCT rat heart are compared in this work.

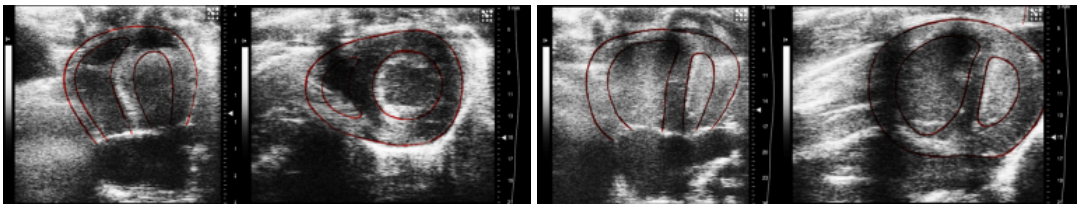

(a) (b)

Figure 1: The long- and short- axis views of the ultrasound images for control (a) and monocrotaline (MCT) rat hearts, respectively. The red curves outline the contours of ventricular walls.

2.2 From image data to rat heart models

3-D finite element bi-ventricular models of the control and MCT rat hearts in Figure 1 are constructed, and rule-based fibre structures are embedded into the geometries with fibre rotation angle form 60° at endocardium to -60° at epicardium. Then, lumped models for pulmonary and systemic circulation systems are attached to the biventricular models in order to provide boundary conditions for diastolic filling and systolic ejection, as shown in Figure 2.

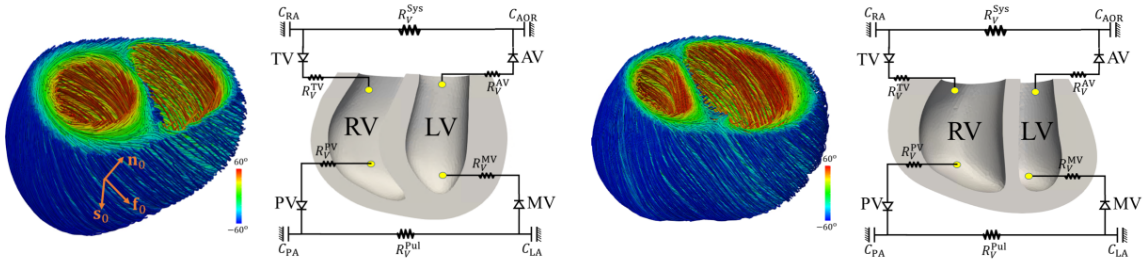

(a) (b)

Figure 2: Schematic illustrations of rat heart model under control (a) and MCT (b) with simple circulation systems and rule-based myofibre structures. $\mathbf{f}_0 - \mathbf{s}_0 - \mathbf{n}_0$ is the local material coordinate system, in which $\mathbf{f}_0$ is the local mean fibre direction, $\mathbf{s}_0$ is the sheet direction, i.e., transmural direction from endocardium to epicardium, and $\mathbf{n}_0$ is the sheet-normal direction.

It is commonly accepted that the myocardium is a fibre reinforced anisotropic material. Three main constituents in myocardium, the ground matrix, myofibres and collagen fibres with the respective volume fractions ϕ_g, ϕ_m and ϕ_c, are considered in this study, and the total passive strain energy function is

$$\Psi = \phi_\mathrm{g}\,\Psi_\mathrm{g} + \phi_\mathrm{m}\,\Psi_\mathrm{m} + \phi_\mathrm{c}\,(\Psi_\mathrm{f} + \Psi_\mathrm{s} + \Psi_\mathrm{n}) \tag{1}$$

where Ψ_g, Ψ_m, Ψ_f, Ψ_s and Ψ_n are the strain energy functions associated with the ground matrix, myofibres, collagen fibres parallel to myofibres and collagen fibres cross to myofibres along sheet and sheet-normal directions, and they are

$$\begin{aligned} \Psi_\mathrm{g} &= \frac{a_\mathrm{g}}{2}(I_1 - 3), \qquad \Psi_\mathrm{m} = \frac{a_\mathrm{m}}{2b_\mathrm{m}}\{\exp[b_\mathrm{m}(I_{4\mathrm{m}} - 1)^2] - 1\}, \\ \Psi_i &= \frac{a_i}{2b_i}\{\exp[b_i(\max(I_{4i}/\lambda_{bc}^2, 1) - 1)^2] - 1\}, \qquad i \in \{\mathrm{f},\,\mathrm{s},\,\mathrm{n}\}, \end{aligned} \tag{2}$$

where I_1 is the trace of right Cauchy–Green deformation tensor, I_{4i} with $i \in \{\text{m, f, s, n}\}$ is the square of fibre stretch along respective direction, and λ_{bc} is activating value, after which collagen fibres begin to contribute. Active contraction is achieved by including active stress $\boldsymbol{\sigma}_a = T_a \hat{\mathbf{m}} \otimes \hat{\mathbf{m}}$, where T_a is the active tension generated by myofibres and $\hat{\mathbf{m}}$ is the unit deformed myofibre direction.

2.3 Estimation of growth between the control and MCT hearts

Here, we estimate the amount of growth from the control heart to the MCT heart. *Deformetrica*[1], an open-source package based on a large deformation diffeomorphic metric mapping framework, is employed to warp the control heart to the MCT heart in Figure 2. A dense displacement field is estimated by minimizing a loss function that measures the distance between the external surfaces of the control (C_α) and MCT (C_β) hearts. After warping C_α into C_β, the displacement field for all nodes on the external surface of C_α is obtained, denoting $\mathbf{u}_{\text{Ex}}$. The displacement vectors on the nodes lying within the ventricular wall are then interpolated by solving a Laplace system with Dirichlet boundary conditions, that is

$$\nabla^2 \mathbf{u} = 0, \quad \text{and} \quad \mathbf{u} = \mathbf{u}_{\text{Ex}} \quad \text{at external surface.} \tag{3}$$

Following the finite deformation theory, the deformation gradient of warping the control heart to the MCT heart is

$$\mathbf{G} = \nabla \mathbf{u} + \mathbf{I}, \tag{4}$$

in which $\mathbf{I}$ is the identity matrix. Note that $\mathbf{G}$ and $\mathbf{u}$ are associated with the control heart, and $J = \det(\mathbf{G})$ represents the volumetric growth amount from the control heart to the MCT heart. Growth amount along each material coordinate is $G_{ij} = \mathbf{G} : \boldsymbol{i}_0 \otimes \boldsymbol{j}_0$ with $i, j \in \{\text{f, s, n}\}$.

3 RESULTS AND CONCLUSIONS

Current numerical simulations can reproduce the main characteristics of cardiac functions of rat hearts under control and MCT states. Figure 3(a) shows the simulated pressure-volume loops of control and MCT rat hearts, in which RV end-systolic pressure increases by 170% from 25 mmHg in the control heart to 67.5 mmHg in the MCT heart. Reduced RV pump function occurs in the MCT heart, halved ejection fraction of RV (26%) compared to that of the control heart (56%) though the stroke volumes are similar (0.15 ml vs 0.16 ml). The MCT heart also has a slightly decreased LV ejection fraction compared to the control heart, 58% vs. 55%, which may be caused by the dilated RV that pushes the septum towards the left side as shown in Figure 1 and thus restrains the diastolic filling of LV.

Growth tensor is estimated by Eq. (4) by comparing the control and MCT hearts, and representative element sets are collected from the LV free wall (LVFW), RVFW and the septum, respectively. Figure 3(b) compares the mean value of each entry of the growth tensor, in which growth mainly occurs along the fibre, sheet and sheet-normal axial directions. LV has balanced growth along three orthogonal axes with a mean volumetric growth amount $\bar{J} = 1.75$, whilst RV grows mainly along the sheet direction, i.e., thickening RVFW with $\bar{J} = 2.7$, followed by the septum with the least growth ($\bar{J} = 1.3$). The septum may have complex growth and remodelling process, as the shear growth components are much bigger than those of LVFW and RVFW.

Existing studies have suggested that mechanical cues (stress and stretch) can play a significant role in pathological myocardial growth [4]. Here, we further carried out the correlation analysis between the mechanical states (the stress σ_{ii} and square of stretch I_{4i} along the material coordinates) and estimated growth quantities (G_{ij}). To determine the mechanical cues, we applied the boundary conditions of the MCT heart to the control heart. Our results demonstrate that growth tensor correlates with fibre stretch and stress well. For example, Figure 3(e) describes the correlation between the square of stretch ($I_{4\text{f}}$) at end of diastole and growth amount along the mean fibre direction at the septum, with the correlation coefficient 0.77 ($p < 0.005$), whilst the correlations are not significant at LVFW and RVFW (Figure 3(c,d)). Figure 3(e) indicates larger fibre stretch at the septum suppresses the growth along the mean fibre direction, different from the published growth rules that larger fibre stretch

[1] `http://www.deformetrica.org/`

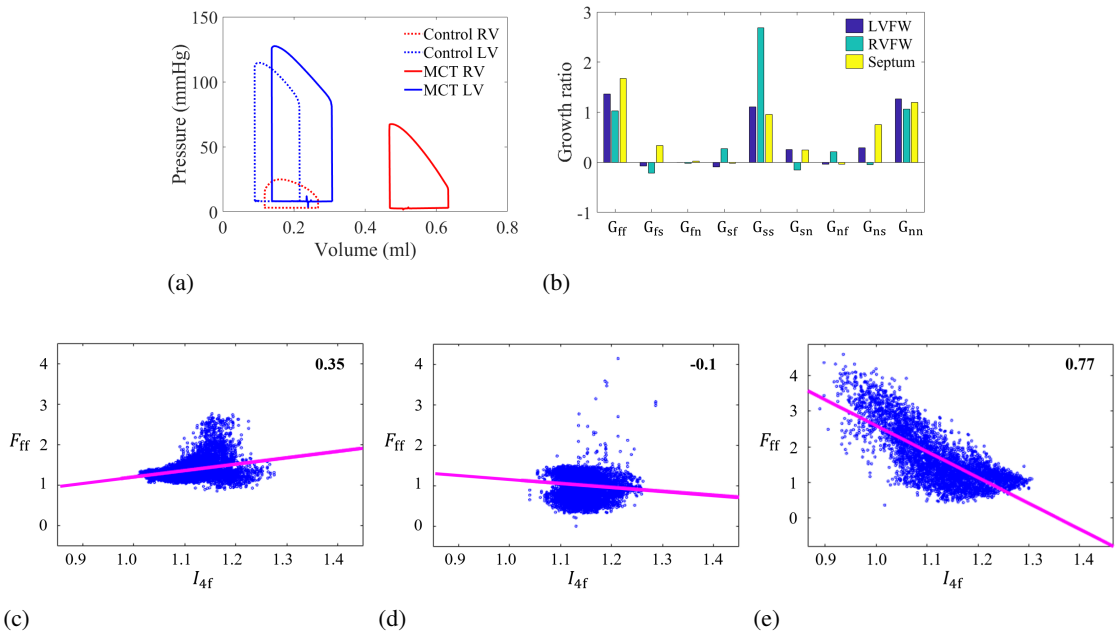

Figure 3: (a) Pressure-volume loops of the Control and MCT rat hearts. (b) Mean value of each entry in growth tensors at LVFW, RVFW and septum, respectively, from the Control shape to the MCT shape. Correlation relationship between square of fibre stretch (I_{4f}) at end of diastole and growth amount along the mean fibre direction at LVFW (c), RVFW (d), and septum (e), respectively.

contributes to bigger growth [4], this may be due to the complex growth tensor in the septum with large shear components.

Our models based on ultrasound image data can achieve physiological cardiac functions under both normal and diseased conditions. The methodology to estimate growth tensor by warping the control heart to the MCT heart provides an achievable approach to quantify growth amount along each material axis. Our results further show myocardial growth not only is spatially heterogeneous but also is correlated with certain mechanical cues. The next work is to develop a high-fidelity G&R rat RV model by combining detailed experiments with advanced mathematical modelling, which can characterize the adaptation of RV structure and function during the progression of PAH.

Acknowledgement We are grateful for the funding provided by the UK EPSRC (EP/T017899/1, EP/S030875/1). D.Guan also acknowledges the funding from the school of mathematics and statistics, University of Glasgow through the EPSRC additional funding for mathematical science.

REFERENCES

[1] Avazmohammadi, R., Mendiola, E. A., Li, D. S., Vanderslice, P., Dixon, R. A. F., and Sacks, M. S.. Interactions between structural remodeling and hypertrophy in the right ventricle in response to pulmonary arterial hypertension. *Journal of biomechanical engineering*, 141(9): 091016, 2019.

[2] Guan, D., Yao, J., Luo, X., and Gao, H.. Effect of myofibre architecture on ventricular pump function by using a neonatal porcine heart model: from DT-MRI to rule-based methods. *Royal Society open science*, 7(4), 191655, 2020.

[3] Tian, L., Xiong, P. Y., Alizadeh, E., Lima, P. D., Potus, F., Mewburn, J., ... and Archer, S. L. Supra-coronary aortic banding improves right ventricular function in experimental pulmonary arterial hypertension in rats by increasing systolic right coronary artery perfusion. *Acta Physiologica*, 229(4), e13483, 2020.

[4] Göktepe, S., Abilez, O. J., Parker, K. K., and Kuhl, E.. A multiscale model for eccentric and concentric cardiac growth through sarcomerogenesis. *Journal of theoretical biology*, 265(3), 433-442, 2010.